Newly scalarization of the Einstein-Euler-Heisenberg black hole

Lina Zhang[1*], De-Cheng Zou[2†] and Yun Soo Myung[3‡]

[1]College of Science, Hunan Institute of Technology, Hengyang 421002, China
[2]College of Physics and Communication Electronics, Jiangxi Normal University, Nanchang 330022, China
[3]Center for Quantum Spacetime, Sogang University, Seoul 04107, Republic of Korea

Abstract

Th spontaneous scalarization of the Einstein-Euler-Heisenberg (EEH) black hole is performed in the EEH-scalar theory by introducing an exponential scalar coupling (with α coupling constant) to the Maxwell term. Here, the EEH black hole as a blad black hole is described by mass M and magnetic charge q with an action parameter μ. A choice of $\mu = 0.3$ gurantees a single horizon with unrestricted magnetic charge q. The onset scalarization of this black hole appears for a positive coupling α with an unlimited magnetic charge q. However, there exists a difference between $q \leq 1$ and $q > 1$ onset scalarizations. We notify the presence of infinite branches labeled by the number of $n = 0, 1, 2, \cdots$ of scalarized charged black holes by taking into account the scalar seeds around the EEH black hole. We find that the $n = 0$ fundamental branch of all scalarized black holes is stable against the radial perturbations, while the $n = 1$ excited branch is unstable.

*e-mail address: linazhang@hnit.edu.cn
†e-mail address: dczou@jxnu.edu.cn
‡e-mail address: ysmyung@inje.ac.kr

1 Introduction

No-hair theorem states that a black hole is completely described by the mass (M), electric charge (Q), and rotation parameter (a) [1]. If a scalar field is minimally coupled to gravitational and electromagnetic fields, it could not survive as an equilibrium configuration around the black hole, which describes no-scalar hair theorem [2].

Introducing nonminimal couplings, however, analytic solutions of black hole with scalar hair have been found. Considering a conformal scalar coupling to the Ricci scalar ($\phi^2 R/6$), the BBMB black hole with secondary scalar hair has been found [3, 4], regarding as an extremal black hole (outer horizon=inner horizon). If one introduces a dilatonic coupling (e^{ϕ}) coupling to the Maxwell term, one obtained the well-known GMGHS black hole solution with secondary dilatonic hair [5, 6, 7, 8], but its inner horizon disappears. These asymptotically flat black hole solytions support the no scalar-haired inner horizon theorem. This theorem implies that there exist no inner (Cauchy) horizons for spherically symmetric black holes with nontrivial scalar (dilaton) hairs [9, 10, 11]. In other words, this states a close connection between scalar hair and inner horizon.

Many black hole solutions with scalar hair were numerically constructed from the Einstein-Gauss-Bonnet-scalar theory [12, 13, 14] and Einstein-Maxwell-scalar (EMS) theory [15] by introducing the nonminimal coupling function $f(\phi)$ to the Gauss-Bonnet term and Maxwell term, respectively [16, 17, 18]. This is called spontaneous scalarization where there is no room to include the inner horizon because they belong to series solutions. It is worth noting that the onset of spontaneous scalarization is surely captured by its linearized scalar theory. This was usually implemented by the tachyonic instability of a linearized scalar around the bald [Schwarzschild and Reissner-Nordström (RN)] black holes without scalar hair. Nowadays, we are getting into the evasion era of the no-hair theorem with the no scalar-haired inner horizon theorem.

In this work, we consider the Einstein-Euler-Heisenberg-scalar (EEHS) theory to investigate the spontaneous scalarization of its EEH black hole with the Euler-Heisenberg parameter μ. In case of $\mu \leq 0.08$ with black hole mass $M = 1$, it is important to note that one could obtain a single horizon with unlimited magnetic charge ($q > 0$), comparing to $q \leq 1$ for RN black hole. Hence, this satisfies the no scalar-haired inner horizon theorem automatically. At this stage, we note that a negative potential-induced scalarization of EEH black hole without any scalar coupling function $f(\phi)$ led to a single branch of unstable

scalarized EEH black holes [19]. Introducing an exponential scalar coupling $f(\phi) = e^{-\alpha\phi^2}$ with a scalar coupling parameter α to the Maxwell term $\mathcal{F}$, the onset scalarization of this black hole occurs for a positive coupling α and an unlimited magnetic charge $q > 0$. In the sutdy of onset scalarization, we introduce three conditions for tachyonic instability with $\alpha \geq \alpha_{\rm i}$: sufficient condition $\alpha_{\rm sEEH}(M, q)$, instability condition $\alpha_{\rm in}(M, q)$, and threshold of instability $\alpha_{\rm th}(M, q)$. Here, the first and second are found analytically but they are approximate quantities, while the latter is obtained by numerically and it is a exact quantity. From $\alpha_{\rm sEEH}(M, q)$ and $\alpha_{\rm in}(M, q)$, one finds a different behavior of the onset scalarization between $q \leq 1$ and $q > 1$. The former is simlar to the onset scalarization of conventional RN black holes, whereas the latter is regarded as a newly scalarization. We stress again that the latter is surely considered as the new domain of spontaneous scalarization when choosing an unlimited magnetic charge $q > 0$. We check the existence of infinite branches ($n = 0, 1, 2, \cdots$) for scalarized charged black holes by studying the scalar seeds around the EEH black holes.

We will obtain scalarized charged black holes for different $q = 0.5, 2, 20$ in the $n = 0$ fundamental branch by solving full equations. The stability of the $n = 0$ branch with respect to radial perturbations will be reached by examining the qualitative behavior of the scalar potentials around the $n = 0$ branch as well as by obtaining exponentially growing (unstable) modes for s-mode scalar perturbation. We expect to find that the $n = 0$ branch is stable, implying that its astrophysical applications might be put to the test.

The organization of the present work is as follows. In section 2, we introduce the EEHS theory and the EEH black holes. In section 3, we study the onset scalarization around the EEH black holes extensively by emplying analytic and nemerical methods to handle the linearized scalar theory. Section 4 is devoted to exploring scalarized EEH black holes with $q = 0.5, 2, 20$ in the $n = 0$ funmadental branch. The stability analysis of the $n = 0, 1$ branches will be performed by introducing the radial perturbations in section 5. Finally, we would like to mention discussions on our results in section 6.

2 EEH black holes

The Einstein-Euler-Heisenberg-scalar (EEHS) action is introduced with an action parameter μ for a nonlinear electrodynamics term $\mathcal{F}^2$

$$S = \frac{1}{16\pi}\int d^4x\sqrt{-g}\Big[R - 2\partial_\mu\phi\partial^\mu\phi - e^{-\alpha\phi^2}\mathcal{F} + \mu\mathcal{F}^2\Big], \tag{1}$$

where α is a scalar coupling constant to the Maxwell term, $\mathcal{F} = F_{\mu\nu}F^{\mu\nu}$.

Before we proceed, we note that scalarized dyonic black holes were obtained from the EMS with an additional quasi-topological term of $\mathcal{F}^2 - 2F^{(4)}$ with $F^{(4)} = F^\mu_\nu F^\nu_\rho F^\rho_\sigma F^\sigma_\mu$ [20] and scalarized Bardeen black holes were recently found from the Einstein-scalar coupling to a nonlinear electrodynamics term $[\frac{(q^2\mathcal{F}/2)^{5/4}}{(1+\sqrt{q^2\mathcal{F}/2})^{5/2}}]$ which provides a regular black hole as a bald one [21]. Their $n = 0$ branches turned out to be stable against radial perturbations.

The Einstein equation can be obtained from the action Eq.(1) under the variation with respect to the metric tensor $g_{\mu\nu}$ as

$$G_{\mu\nu} = 2\Big[\partial_\mu\phi\partial_\nu\phi - \frac{1}{2}(\partial\phi)^2 g_{\mu\nu} + T_{\mu\nu}\Big], \tag{2}$$

where the energy-momentum tensor is given by

$$T_{\mu\nu} \;=\; e^{-\alpha\phi^2}\Big(F_{\mu\rho}F_\nu{}^\rho - \frac{1}{4}\mathcal{F}g_{\mu\nu}\Big) - 2\mu\Big(\mathcal{F}F_{\mu\rho}F^\rho_\nu - \frac{1}{8}\mathcal{F}^2 g_{\mu\nu}\Big). \tag{3}$$

The Maxwell equation takes the form

$$\nabla_\mu(F^{\mu\nu} - 2\mu\mathcal{F}F^{\mu\nu}) = 2\alpha\phi\nabla_\mu(\phi)F^{\mu\nu}. \tag{4}$$

On the other hand, the scalar equation involes an effective mass term due to the nonminimal scalar coupling to the Maxwell term as

$$\nabla^2\phi + \frac{\alpha}{2}\mathcal{F}e^{-\alpha\phi^2}\phi = 0. \tag{5}$$

Introducing the mass function $\bar{m}(r)$ together with the gauge field $\bar{A}_{\hat{\varphi}} = -q\cos\theta$ and the hairless scalar $\bar{\phi} = 0$, one finds the Einstein equation

$$\bar{m}'(r) = \frac{q^2}{2r^2} - \mu\frac{q^4}{r^6}. \tag{6}$$

Its spherically symmetric solution is given by the EEH black hole [22, 23, 24, 25] as

$$ds^2 = \bar{g}_{\mu\nu}dx^\mu dx^\nu = -f(r)dt^2 + \frac{dr^2}{f(r)} + r^2 d\Omega_2^2, \tag{7}$$

where the metric function takes the form with the Maxwell term

$$f(r) \equiv 1 - \frac{2\bar{m}(r)}{r} = 1 - \frac{2M}{r} + \frac{q^2}{r^2} - \frac{2\mu q^4}{5r^6}, \quad \bar{\mathcal{F}} = \frac{2q^2}{r^4}. \tag{8}$$

It is meaningful to note that the EEH black hole contains three parameters $\{M, q, \mu\}$. Here, M represents the ADM mass, q denotes the magnetic charge, and μ is the action parameter. In case of $\mu \leq 0.08$ with $M = 1$, it was shown that there exist three horizons with one point at $q = 0$ [26], leading to a complicated analysis. In the present work, it would be better to introduce a single horizon which satisfies the no scalar-haired inner horizon theorem automatically [9]. If one chooses $\mu = 0.3$ appropriately, one finds the single horizon. In (Right) Fig. 1, we represent three metric functions $f(r, M = 1, q, \mu = 0.3)$ as functions of $r \in [0.5, 20]$ with $q = 0.5, 2, 20$. They cross r-axis at $r = 1.87(q = 0.5), 0.89(q = 20), 2.63(q = 20)$, which represent the event horizons $r_+(M = 1, q)$ at $q = 0.5, 2, 20$.

As is shown in (Left) Fig. 1, we display the single horizon $r_+(M = 1, q)$ to $f(r) = 0$. It is worth noting that there is no theoretical constraint on restricting the magnetic charge q and thus, $r_+(1, q)$ becomes a continuous function of q: it takes the minimum of $r_+(1, 1.39) = 0.83$ and then, it is an increasing function of q with $r_+(1, q = 100) = 5.88$. It differs quitely from the well known RN black hole ($\mu = 0$ case) possessing outer/inner horizons $r_{RN\pm}(M = 1, q) = 1 \pm \sqrt{1 - q^2}$ and having a confined region of $q \in [0, 1]$. We note $r_+(1, q)$ and $r_{RN+}(1, q)$ are similar to each other only for $q \in [0, 1]$.

3 Onset of spontaneous scalarization

To study the onset of spontaeous scalarization, we need to introduce the linearized scalar theory. The linearized metric theory was used to perform the stability of EEH black holes [27]. If one introduces a scalar perturbation around the EEH black hole background as

$$\phi = 0 + \delta\varphi, \tag{9}$$

its linearized scalar equation is given by

$$\Big(\bar{\nabla}^2 + \frac{\alpha q^2}{r^4}\Big)\delta\varphi = 0. \tag{10}$$

For our purpose, we introduce the separation of variables

$$\delta\varphi(t, r, \theta, \hat{\phi}) = \varphi(r) Y_{lm}(\theta) e^{im\hat{\phi}} e^{-i\omega t}, \quad \varphi(r) = \frac{u(r)}{r}. \tag{11}$$

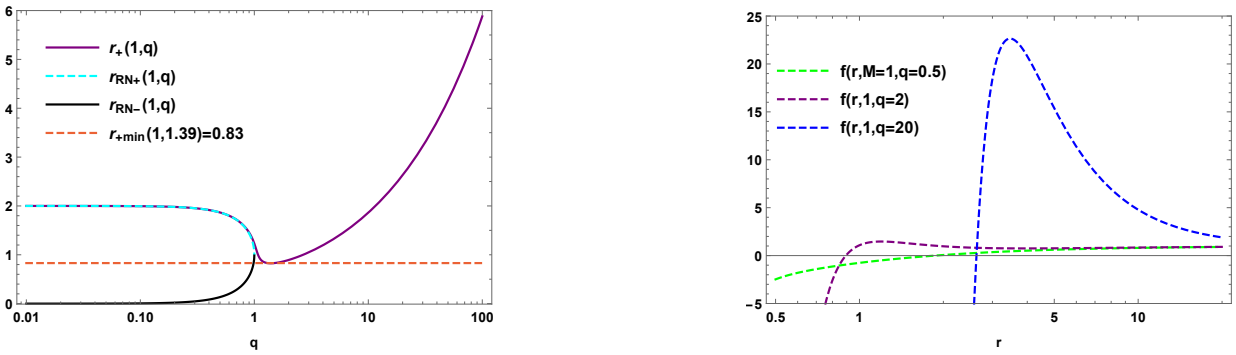

Figure 1: (Left) Two outer horizons $r_+(1,q) > r_{\rm RN+}(1, q \in [0,1])$ with an inner horizon $r_{RN-}(1, q \in [0,1])$. $r_+(1,q)$ has the minimum of $r_+(1,1.39) = 0.83$ and then, it is an increasing function of q. We note $r_+(1,100) = 5.88$. (Right) Metric functions $f(r, M = 1, q, \mu = 0.3)$ as functions of $r \in [0.5, 20]$ with $q = 0.5, 2, 20$. They cross r-axis at $r = 1.87(q = 0.5),\ 0.89(q = 2),\ 2.63(q = 20)$, representing three event horizons $r_+(M = 1, q)$ at $q = 0.5, 2, 20$.

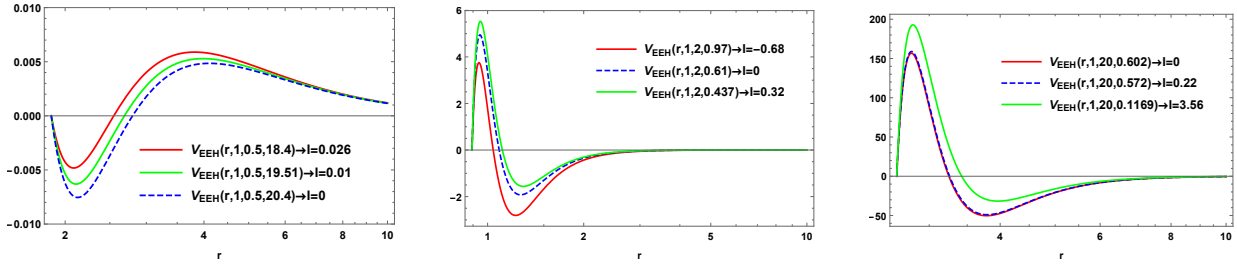

Figure 2: Potential $V_{\rm EEH}(r, M = 1, q, \alpha)$ and its integration $I(M = 1, q, \alpha)$ with $q = 0.5, 2, 20$. (Left) Three α-dependent potentials $V_{\rm EEH}(r, M = 1, q = 0.5, \alpha)$ as functions of $r \in [r_+(1, 0.5) = 1.866, 10]$ with $\alpha = 18.4(= \alpha_{\rm in}),\ 19.51(= \alpha_{\rm th}),\ 20.4(= \alpha_{\rm sEEH})$. (Middle) Three potentials $V_{\rm EEH}(r, 1, q = 2, \alpha)$ as functions of $r \in [r_+(1, 2) = 0.893, 5]$ with $\alpha = 0.437(= \alpha_{\rm th}),\ 0.61(= \alpha_{\rm sEEH}),\ 0.97(= \alpha_{\rm in})$. (Right) Three potentials $V_{\rm EEH}(r, 1, q = 20, \alpha)$ as functions of $r \in [r_+(1, 20) = 2.63, 10]$ with $\alpha = 0.1169(= \alpha_{\rm th}),\ 0.572(= \alpha_{\rm in}),\ 0.602(= \alpha_{\rm sEEH})$. If $q > 1.14, 17.5$, their roles of $\alpha_{\rm in}$, $\alpha_{\rm th}$, and $\alpha_{\rm sEEH}$ are exchanged.

In coorperation with the tortoise coordinate $r_* = \int \frac{dr}{f(r)}$, Eq. (10) is converted into the Schrödinger equation for $u(r)$

$$\frac{d^2u(r)}{dr_*^2} + \Big[\omega^2 - V_{\rm EEH}(r, M, q, \alpha)\Big]u(r) = 0, \tag{12}$$

where the $s(l=0)$-mode potential is given by

$$V_{\rm EEH}(r,M,q,\alpha) = f(r)\Big[\frac{2M}{r^3}-\frac{(2+\alpha)q^2}{r^4}+\frac{3.6q^4}{5r^8}\Big] \to f(r)\cdot v_{\rm EEH}(r). \tag{13}$$

See Fig. 2, for its α-dependent potential forms $V_{\rm EEH}(r,M=1,q,\alpha)$ with $q=0.5,2,20$.

We wish to compute three quantities of coupling constant α: sufficient condition $\alpha_{\rm sEEH}(1,q)$, instability condition $\alpha_{\rm in}(1,q)$, and threshold of instability $\alpha_{\rm th}(1,q)$, where the first two are approximate results obtained from the scalar potential analytically, while the last is the exact value determined either by solving Eq.(12) with $\omega=i\Omega$ or by solving the static linearized equation numerically.

First of all, it is easy to compute the sufficient condition for tachyonic instability given by [28]

$$\int_{r_+(M,q)}^{\infty}\Big[\frac{V_{\rm EEH}(r)}{f(r)}\Big]dr \to \int_{r_+(M,q)}^{\infty} v_{\rm EEH}(r)dr \equiv I<0 \tag{14}$$

which determines the upper bound of $\alpha_{\rm sEEH}(M,q)$ in the instability condition for $q<1.14$

$$\alpha_{\rm in}(M,q)<\alpha_{\rm th}(M,q)<\alpha_{\rm sEEH}(M,q). \tag{15}$$

This sequency of instability is usually suitable for the onset scalarization of RN black holes found in the EMS theory [16]. On the other hand, one finds other sequency of the inequality for $1.14<q<17.5$

$$\alpha_{\rm th}(M,q)<\alpha_{\rm sEEH}(M,q)<\alpha_{\rm in}(M,q). \tag{16}$$

In addition, for $q>17.5$, one obtains another sequency of the inequality as

$$\alpha_{\rm th}(M,q)<\alpha_{\rm in}(M,q)<\alpha_{\rm sEEH}(M,q). \tag{17}$$

It is worth noting that Eqs.(16) and (17) are new and appear for the onset of spontaneous scalarization in the EEH black holes with unlimited magentic charge q. (Left) Fig. 2 for $q=0.5$ implies that the threshold of instability $\alpha_{\rm th}(1,0.5)=19.51$ is between $\alpha_{\rm in}=18.4$ and $\alpha_{\rm sEEH}=20.4$. Differently, we observe α-dependent potentials for $q=2,20$ as shown in (Middle/Right) Fig. 2. Also, we observe that"$-+$" regions appear in the near-horizon for $q=0.5$, while "$+-$" regions are shown in the near-horizon for $q=2,15$.

At this stage, we present explicit forms $\alpha_{\rm sEEH}(M=1,q)$ and $\alpha_{\rm sRN}(M=1,q)$ [16] obtained from the sufficient condition of $I=0$ as

$$\alpha_{\rm sEEH}(1,q\in[0,\infty]) = -2+\frac{3r_+(1,q)}{q^2}+\frac{0.31q^2}{r_+^4(1,q)}, \tag{18}$$

$$\alpha_{\rm sRN}(1,q\in[0,1]) = -2+\frac{3r_{\rm RN+}(1,q)}{q^2}, \tag{19}$$

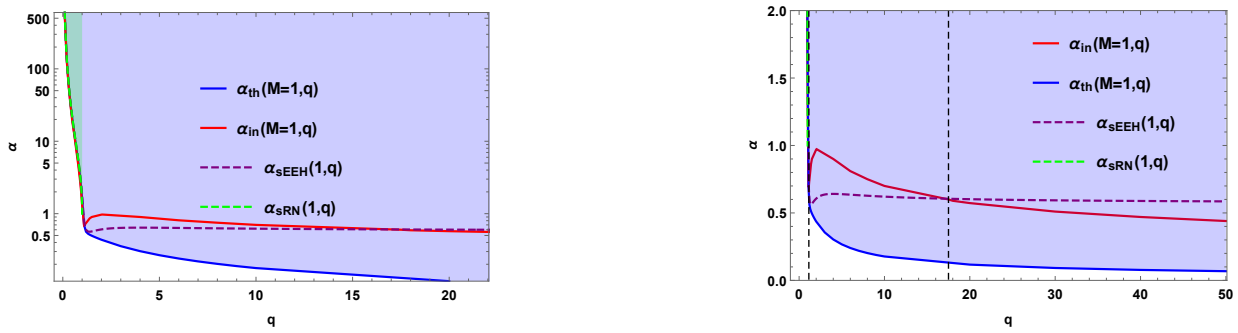

Figure 3: (Left) Sufficient condition for tachyonic instability $\alpha_{\rm sEEH}(1,q)$, threshold of instability $\alpha_{\rm th}(1,q)$, and instability condition $\alpha_{\rm in}(1,q)$ as functions of $q \in [0,22]$ with $\alpha_{\rm sRN}(1, q \in [0,1])$. It implies a conventional inequality of $\alpha_{\rm in} \leq \alpha_{\rm th} \leq \alpha_{\rm sEEH}$ for the green shaded region ($q \in [0,1]$). The whole shaded region represents unstable region of $\alpha(1,q) \geq \alpha_{\rm th}(1,q)$. (Right) Their enlarged picture for $\alpha \in [0,2]$. One finds positive regions for α with two dashed lines at $q = 1.14, 17.5$ (crossing points), $\alpha_{\rm sEEH}(1,1000) = 0.58$, and $\alpha_{\rm in}(1,1000) = 0.22$. One expects to have other inequality of $\alpha_{\rm th} \leq \alpha_{\rm sEEH} \leq \alpha_{\rm in}$ for $1.14 < q < 17.5$, while $\alpha_{\rm th} \leq \alpha_{\rm in} \leq \alpha_{\rm sEEH}$ for $q > 17.5$.

which are depicted in (Left) Fig. 3. It is important to realize that $\alpha_{\rm sEEH}(1,q)$ is a decreasing function of q, but it crosses $\alpha_{\rm in}$ at $q = 1.14, 17.5$ which is a new feature for the onset of spontaneous scalarization [see (Right) Fig. 3]. Hence, we choose $q = 0.5, 2, 20$ for real computations. Importantly, we observe that for $\alpha \leq 1$, the predictions of $\alpha_{\rm sEEH}(1,q)$ and $\alpha_{\rm in}(1,q)$ are quite diffrent from that for threshold of intability $\alpha_{\rm th}(1,q)$, which implies that two formers may not be suitable for studying the instability of EEH black holes. However, for $\alpha > 1$, three of $\alpha_{\rm sEEH}(1,q)$, $\alpha_{\rm in}(1,q)$, $\alpha_{\rm th}(1,q)$ with $\alpha_{\rm sRN}(1,q)$ predict the nearly same behavior.

To obtain the instability condition $\alpha_{\rm in}(M,q)$, the spatially regular scalar configurations (scalar clouds) can be obtained from Eq.(12) with $\omega = 0$ by adopting the WKB technique [29]. A second-order WKB method could be applied for obtaining the bound states of the potential $V_{\rm EEH}(r_*)$ approximately to yield the quantization condition

$$\int_{r_*^{\rm in}}^{r_*^{\rm out}} dr_* \sqrt{-V_{\rm EEH}(r_*)} = \Big(n - \frac{1}{4}\Big)\pi, \quad n = 1, 2, 3, \cdots, \tag{20}$$

where $r_*^{\rm out}$ and $r_*^{\rm in}$ are the radial turning points satisfying $V_{\rm EEH}(r_*^{\rm out}) = V_{\rm EEH}(r_*^{\rm in}) = 0$. We

may express Eq.(20) in terms of the radial coordinate r as

$$\int_{r_{\rm in}}^{r_{\rm out}} dr \frac{\sqrt{-V_{\rm EEH}(r)}}{f(r)} = \Big(n - \frac{1}{4}\Big)\pi, \quad n = 1, 2, 3, \cdots . \tag{21}$$

Here, radial turning points $(r_{\rm out}, r_{\rm in})$ are determined by the two conditions

$$f(r_{\rm in}) = 0, \quad \frac{2M}{r_{\rm out}^3} - \frac{(\alpha+2)q^2}{r_{\rm out}^4} + \frac{3.6q^4}{5r_{\rm out}^8} = 0, \tag{22}$$

which imply

$$r_{\rm in} = r_+(M, q), \quad r_{\rm out} \simeq \frac{(\alpha+2)q^2}{2M}. \tag{23}$$

For large $\alpha(r_{\rm out})$, the WKB integral (21) is approximated by considering the last term in (13) as

$$\sqrt{\alpha}\cdot q \int_{r_+}^{\infty} \frac{dr}{r^2\sqrt{f(r)}} \equiv \sqrt{\alpha} I_n(M, q) = \Big(n + \frac{3}{4}\Big)\pi, \quad n = 0, 1, 2, \cdots , \tag{24}$$

which could be integrated numerically to yield

$$\alpha_{\rm in,n}(M, q) = \Big[\frac{\pi(n + 3/4)}{I_n(M, q)}\Big]^2, \quad n = 0, 1, 2, \cdots . \tag{25}$$

We plot $\alpha_{\rm in}(M = 1, q)[\equiv \alpha_{\rm in,n=0}(1, q)]$ in Fig. 3, which is the lower bound in Eq.(15) for $q < 1.14$ as well as the upper bound in Eq.(17) for $1.14 < q < 17.5$. It is noted that $\alpha_{\rm in}(1, q)[\simeq \alpha_{\rm sEEH}(1, q)]$ is a decreasing function of q and others of $\alpha_{\rm in,n\neq 0}(1, q)$ are used to estimate branch points. For example, one has $\alpha_{\rm in,0}(1, 0.5) = 18.4$, $\alpha_{\rm in,1}(1, 0.5) = 100$, and $\alpha_{\rm in,2}(1, 0.5) = 247$, which are similar to exact branch points of $\alpha_0 = 19.51$, $\alpha_1 = 101.4$, and $\alpha_2 = 248.73$ for $q = 0.5$ obtained from the static linearized equation.

To determine the threshold of tachyonic instability $\alpha_{\rm th}(M, q)$ lastly, we have to solve the second-order differential equation (12). This allows an exponentially growing mode of $e^{\Omega t}(\omega_i = \Omega > 0)$ as an unstable mode for $\omega = \omega_r + i\omega_i$ with $\omega_r = 0$. Here, we choose two boundary conditions: a normalizable solution of $u(\infty) \sim e^{-\Omega r_*}$ at infinity and a power solution of $u(r_+) \sim (r - r_+)^{\Omega r_+}$ near the outer horizon. We find from (Left) Fig. 4 that the threshold $(\Omega = 0)$ of instability can be determined as $\alpha_{\rm th}(M = 1, q) = 19.51(q = 0.5),\ 0.437(2),\ 0.1169(20)$. Similarly, one obtains $\alpha_{\rm th}(1, q)$ from $q = 0.1$ to $q = 50$ as shown in Fig. 3. This implies that the EEH black hole is unstable for $\alpha(1, q) \geq \alpha_{\rm th}(1, q)$ precisely, while it is stable for $\alpha(1, q) < \alpha_{\rm th}(1, q)$. It is worth mentioning that two of $\alpha_{\rm sEEH}(1, q)$ and $\alpha_{\rm in}(1, q)$ obtained analytically are regarded as approximate results.

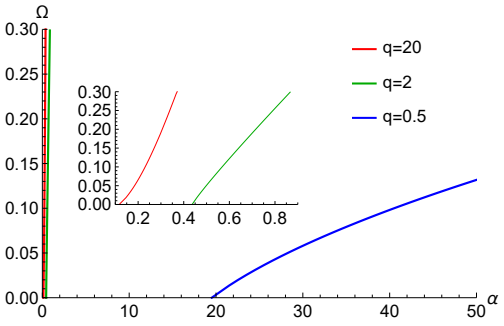

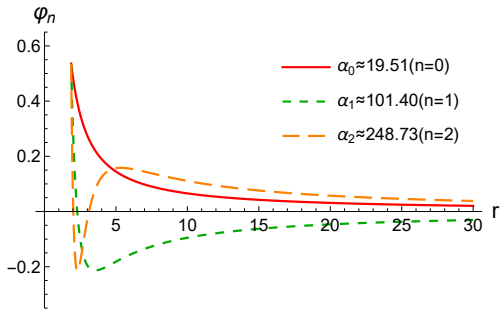

Figure 4: (Left) Three curves of Ω in $e^{\Omega t}$ as a function of α are used to determine the thresholds of tachyonic instability $[\alpha_{\rm th}(1,q)]$ around the EEH black holes. We find that $\alpha_{\rm th}(1,q) = 19.51(q=0.5),\ 0.437(2),\ 0.1169(20)$ when three curves cross α-axis. (Right) $\varphi(r) = u(r)/r$ as a function of $r \in [r_+ = 1.87, 30]$ for representing the first three scalar seeds with $q = 0.5$. $\varphi_n(r)$ is classified by the order number $n = 0, 1, 2$ which is also identified by the number of nodes (zero crossings).

In addition, the other way of getting $\alpha_{\rm th}(1,q)$ is to solve the static linearized equation directly. Also, this can be used to find the scalar seeds $[\varphi_n(r)]$ for $n = 0,\ 1,\ 2, \cdots$ branches of scalarized EEH black holes. We consider the static linearized equation for $\varphi(r)$ around the EEH black hole background

$$\frac{1}{r^2}\Big(r^2 f(r)\varphi'(r)\Big)' - \Big(\frac{l(l+1)}{r^2} - \frac{\alpha q^2}{r^4}\Big)\varphi(r) = 0, \tag{26}$$

which describes an eigenvalue problem. For $l = 0$, requiring an asymptotically vanishing scalar $[\varphi(r \to \infty) = 0]$ imply that a smooth scalar selects a discrete set of $n = 0,\ 1,\ 2, \cdots$. Also, it determines the bifurcation points $[\alpha_n(1,q)]$ precisely. First of all, it is confirmed that $\alpha_{\rm th}(1, 0.5) = \alpha_0(1, 0.5)$. We plot scalar seeds $\varphi_n(r)$ with $q = 0.5$ as a function of r for three branches of $n = 0(\alpha_0 = 19.51),\ n = 1(\alpha_1 = 101.40),\ n = 2(\alpha_2 = 248.73)$ [see (Left) Fig. 4]. It is important to note that the scalar seed $\varphi_0(r)$ without zero crossing will develop the scalar hair $\phi_0(r)$ which describes the $n = 0$ fundamental branch of scalarized charged black holes for $\alpha \geq \alpha_0 (= \alpha_{\rm th})$. On the other hand, two scalar seeds $\varphi_1(r)$ and $\varphi_2(r)$ with zero crossings will develop the scalar hairs $\phi_1(r)$ and $\phi_2(r)$ which describe $n = 1$ and $n = 2$ excited branches of scalarized charged black holes existing for $\alpha \geq \alpha_1$ and $\alpha \geq \alpha_2$. In general, infinite branches of $n = 0,\ 1,\ 2, \cdots$ can be constructed from infinite α-bounds

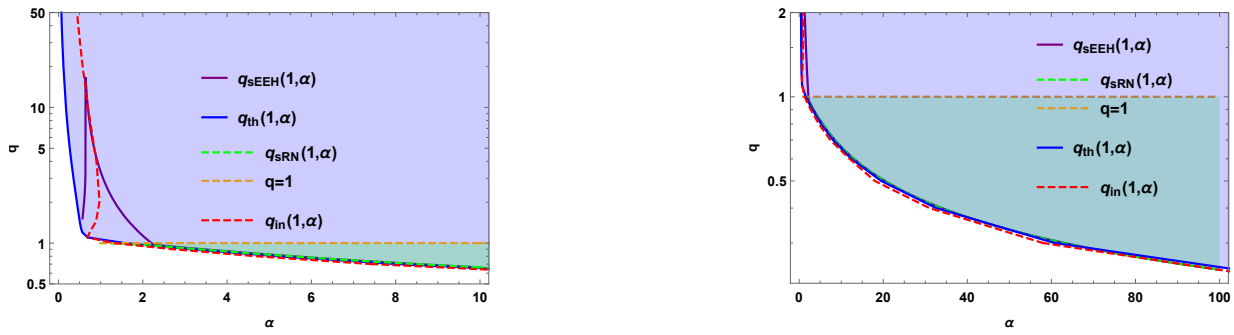

Figure 5: (Left) Existence curves $q_{\rm sEEH}(1,\alpha)$, $q_{\rm th}(1,\alpha)$, and $q_{\rm in}(1,\alpha)$. The green shaded region $[q_{\rm sRN}(1,\alpha) \leq q(1,\alpha) \leq 1]$ denotes a convential existence region for RN black hole. The whole shaded region represents existence region of $q(1,\alpha) \geq q_{\rm th}(1,\alpha)$, implying unlimited magenetic charge q. (Right) Their enlarged picture for $\alpha \in [0,100]$ vs $q \in [0,2]$.

of $\alpha \geq \alpha_0$, $\alpha \geq \alpha_1$, $\alpha \geq \alpha_2$, $\cdots$, respectively. This describes briefly a prescription for obtaining infinite branches of scalarized EEH black holes.

Finally, we wish to display the existence region for scalarized EEH black holes based on $q_{\rm th}(M=1,\alpha)$ in Fig. 5 . Here, $q_{\rm sRN}(1,\alpha>1) = \frac{\sqrt{3+6\alpha}}{\alpha+2}$ is found from the condition of $I_{\rm RN}=0$ for q, while $q_{\rm sEEH}(1,\alpha \geq 0.57)$ is obtained from the condition of $I=0$ for q, it takes the maximum (=15.2) at $\alpha=0.65$ and then, it is a monotonically decreasing function of α. $q_{\rm th}(1,\alpha)$ and $q_{\rm in}(1,\alpha)$ are the inverse functions of $\alpha_{\rm th}(1,q)$ and $\alpha_{\rm in}(1,q)$, respectively. For $q>1$, $q_{\rm th}(1,\alpha)$, $q_{\rm sEEH}(1,\alpha)$, and $q_{\rm in}(1,\alpha)$ indicate different predictions. Explicitly, the predictions of $q_{\rm sEEH}(1,\alpha)$ and $q_{\rm in}(1,\alpha)$ are quite diffrent from that for threshold of intability $q_{\rm th}(1,\alpha)$, implying that two formers are not appropriate for determing the existence region for scalarized EEH black holes.

For $q \leq 1$, however, three of $q_{\rm th}(1,\alpha)$, $q_{\rm sEEH}(1,\alpha)$, and $q_{\rm in}(1,\alpha)$ with $q_{\rm RN}(1,\alpha)$ predict the nearly same behavior. The whole shaded region corresponds to the existence (unstable) region for scalarized EEH black holes without the limitation on the magnetic charge q. It includes a convential existence (unstable) region for RN black hole [green shaded region between $q_{\rm sRN}(1,\alpha)$ and 1].

4 Scalarized EEH black holes

All scalarized EEH black holes can be generated from the onset of scalarization $\{\varphi_n(r)\}$ in the unstable region of EEH black holes $[\alpha(1,q) \geq \alpha_{\rm th}(1,q)]$. It is clear that the scalarized black hole solutions arise dynamically from the evolution of EEH black hole when scalar cloud $\varphi_n(r)$ plays the role of a seed for n-branch.

We wish to obtain scalarized EEH black holes through spontaneous scalarization by solving full equations. To this direction, one considers the metric and field ansatzes as [15]

$$\begin{aligned} ds^2_{\rm sEEH} &= -N(r)e^{-2\delta(r)}dt^2 + \frac{dr^2}{N(r)} + r^2(d\theta^2 + \sin^2\theta d\hat{\varphi}^2) \\ N(r) &= 1 - \frac{2m(r)}{r}, \quad \phi = \phi(r), \quad A = A_{\hat{\varphi}} d\hat{\varphi}. \end{aligned} \tag{27}$$

Plugging the gauge field ansatz into Eq.(4), one finds a magnetic potential $A_{\hat{\varphi}} = -q\cos\theta$, which implies $F_{\theta\hat{\varphi}} = q\sin\theta$ and $\mathcal{F} = 2q^2/r^4$. This means that it is unnecessary to consider an approximate solution for $A_{\hat{\varphi}}$.

Substituting (27) into Eqs.(2) and (5) leads to three coupled equations for $m(r),\ \delta(r),\ \phi(r)$ as

$$q^2 e^{-\alpha\phi^2(r)} - \frac{2\mu q^4}{r^4} - 2r^2 m'(r) + r^3\left(r - 2m(r)\right)\phi'^2(r) = 0, \tag{28}$$

$$\delta'(r) + r\phi'^2(r) = 0, \tag{29}$$

$$\begin{aligned} &\frac{\alpha q^2 \phi(r) e^{-\alpha\phi^2(r)}}{r^2} - 2[m(r) + rm'(r) - r]\phi'(r) \\ &\quad -r(r-2m(r))[\delta'(r)\phi'(r) - \phi''(r)] = 0. \end{aligned} \tag{30}$$

It is checked that Eq.(28) reduces to Eq.(6) for $\phi(r) = 0$. Assuming the existence of a single horizon located at $r = r_+$, an approximate solution to Eqs.(28)-(30) takes the form in the near horizon as

$$m(r) = \frac{r_+}{2} + m_1(r - r_+) + \cdots, \tag{31}$$

$$\delta(r) = \delta_0 + \delta_1(r - r_+) + \cdots, \tag{32}$$

$$\phi(r) = \phi_0 + \phi_1(r - r_+) + \cdots. \tag{33}$$

Here, the three coefficients are determined by

$$m_1 = \frac{e^{-\alpha\phi_0^2}q^2}{2r_+^2} - \frac{\mu q^4}{r_+^6}, \quad \delta_1 = -r_+\phi_1^2, \quad \phi_1 = \frac{\alpha\phi_0 q^2}{r_+[q^2 - e^{\alpha\phi_0^2}(2\mu q^4/r_+^4 + r_+^2)]}. \tag{34}$$

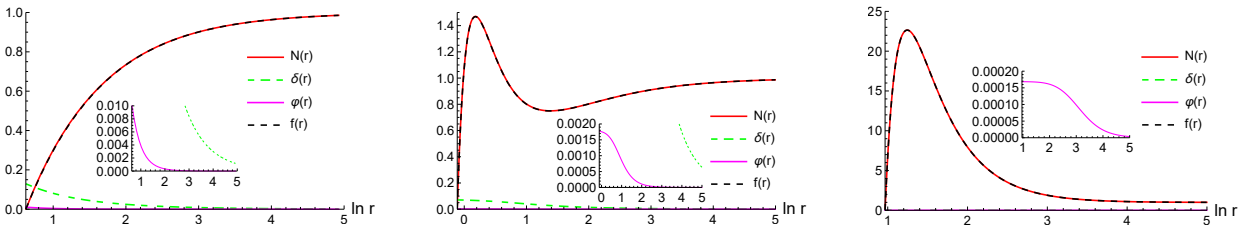

Figure 6: Graph of scalarized EEH black hole solutions. It shows metric functions $N(r)$, $\delta(r)$, and scalar hair $\phi(r)$. Here, $f(r)$ represents metric function for EEH black holes as was shown in (Right) Fig. 1. (Left) $q = 0.5$, and $\ln r_+ = 0.624$ for $\alpha = 25$ in the $n = 0$ branch of $\alpha \geq 19.51$. (Middle) $q = 2$, and $\ln r_+ = -0.1125$ for $\alpha = 0.438$ in the $n = 0$ branch of $\alpha \geq 0.437$. (Right) $q = 20$, and $\ln r_+ = 0.967$ for $\alpha = 0.117$ in the $n = 0$ branch of $\alpha \geq 0.1169$.

Also, two parameters of $\phi_0 = \phi(r_+, \alpha)$ and $\delta_0 = \delta(r_+, \alpha)$ at the outer horizon will be determined when matching with an asymptotically flat solution existing in the far region

$$m(r) = M - \frac{q^2 + q_s^2}{2r} + \cdots, \quad \delta(r) = \frac{q_s^2}{2r^2} + \cdots, \quad \phi(r) = \frac{q_s}{r} + \cdots, \tag{35}$$

where q_s represents a primary scalar charge, M is ADM mass M, and q denotes the magnetic charge.

To obatin scalarized black hole solutions, we use the shooting metod to connect the near horizon solutions with the asymptotic solutions. Regarding as explicit scalarized charged black hole solutions, we present three numerical black hole solutions with $q = 0.5, 2, 20$ in the $n = 0$ fundamental branch in Fig 6. Each $N(r)$ traces out its EEH metric function $f(r)$ for $q = 0.5, 2, 20$ [see (Right) Fig. 1]. Also, we find different values for the scalar hair depending on q at the horizon. Further, it needs to explore hundreds of numerical solutions for different α in the $n = 0, 1$ branches to perform the stability of scalarized charged black holes.

5 Stability for the $n = 0, 1$ branches

It is noted that the stability analysis for scalarized charged black holes is an important task since it determines their viability in representing realistic astrophysical configurations.

The conclusions about the stability of the scalarized charged black holes with respect to perturbations will be reached by examining the qualitative behavior of the potential as well as by obtaining exponentially growing (unstable) modes for s-mode scalar perturbation. It is known that the $n = 0$ fundamental branch is stable agaist radial perturbations, while the exicted ($n = 1, 2$) branches are unstable in the EMS theory [30].

Hence, we prefer to introduce the radial perturbations around the scalarized black holes as

$$\begin{aligned} ds^2_{\rm rp} &= -N(r)e^{-2\delta(r)}(1+\epsilon H_0)dt^2 + \frac{dr^2}{N(r)(1+\epsilon H_1)} + r^2(d\theta^2 + \sin^2\theta d\hat{\varphi}^2), \\ \phi(t,r) &= \phi(r) + \epsilon\delta\tilde{\phi}(t,r), \end{aligned} \tag{36}$$

where $N(r)$, $\delta(r)$, and $\phi(r)$ represent a scalarized charged black hole background, whereas $H_0(t,r)$, $H_1(t,r)$, and $\delta\tilde{\phi}(t,r)$ denote three perturbed fields around the scalarized black hole background. Here, we do not need to introduce a perturbation for the gauge field $A_{\hat{\varphi}}$. From now on, we focus on the $l = 0$(s-mode) scalar propagation by mentioning that higher angular momentum modes ($l \neq 0$) are neglected. In this case, other two perturbed fields become redundant fields. When looking for a decoupling process by using linearized equations, one may find a linearized scalar equation.

Considering the separation of variables

$$\delta\tilde{\phi}(t,r) = \frac{\tilde{\varphi}(r)e^{\Omega t}}{r}, \tag{37}$$

we obtain the Schrödinger-type equation for an s-mode scalar perturbation

$$\frac{d^2\tilde{\varphi}(r)}{dr_*^2} - \Big[\Omega^2 + V_{\rm sEEH}(r,q,\alpha)\Big]\tilde{\varphi}(r) = 0, \tag{38}$$

with r_* is the tortoise coordinate defined by

$$\frac{dr_*}{dr} = \frac{e^{\delta(r)}}{N(r)}. \tag{39}$$

Here, its potential reads to be

$$\begin{aligned} V_{\rm sEEH}(r,q,\alpha) = \frac{e^{-2\delta(r)-\alpha\phi^2(r)}\,N(r)}{r^8}\Big[&e^{\alpha\phi^2(r)}r^6 - q^2r^4 - q^2r^4\alpha + 2e^{\alpha\phi^2(r)}q^4\mu \\ &-e^{\alpha\phi^2(r)}r^6N(r) + 2q^2r^4\alpha^2\phi^2(r) - 4q^2r^5\alpha\phi(r)\phi'(r) + q^2r^6\phi'^2(r) \\ &- 2e^{\alpha\phi^2(r)}r^8\phi'^2(r) - 2e^{\alpha\phi^2(r)}q^4r^2\mu\phi'^2(r)\Big]. \end{aligned} \tag{40}$$

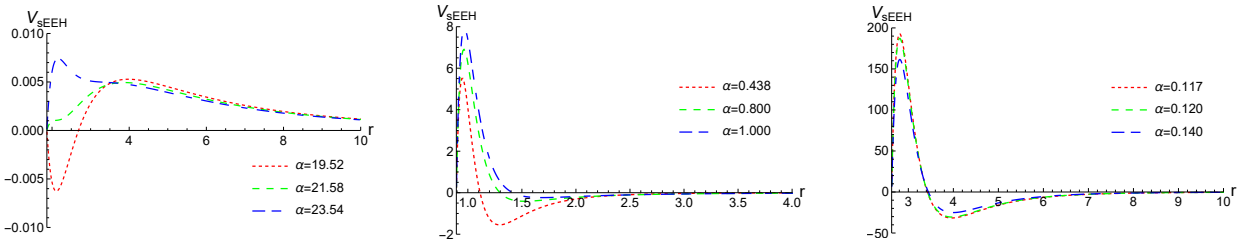

Figure 7: (Left) Three scalar potentials $V_{\rm sEEH}(r, q = 0.5, \alpha)$ for $\alpha = 19.52, 21.58, 23.54$ around the $n = 0$ branch. (Middle) Three scalar potentials $V_{\rm sEEH}(r, q = 2, \alpha)$ for $\alpha = 0.438, 0.8, 1$. (Right) Three scalar potentials $V_{\rm sEEH}(r, q = 20, \alpha)$ for $\alpha = 0.117, 0.12, 0.14$. Even though they contain small negative regions in the near horizon, these turn out to be stable black holes.

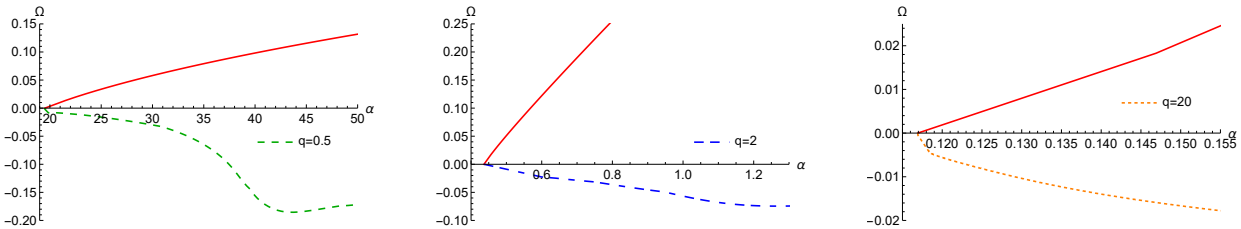

Figure 8: Negative Ω is given as a function of α for the $l = 0$ scalar mode around the $n = 0$ branch, showing stability. Here, we consider three different cases of $q = 0.5$, 2, and 20. Three dotted curves start from $\alpha_{n=0} = 19.51(q = 0.5)$, $0.437(q = 2)$, and $0.1169(q = 20)$. Three red lines represent the unstable EEH black holes [see (Left) Fig. 4].

We check that $V_{\rm sEEH}(r, q, \alpha)$ with $\delta(r) = \phi(r) = 0$ and $N(r) \to f(r)$ reduces to $V_{\rm EES}(r, M, q, \alpha)$ in Eq.(13). At this stage, we wish to observe the potential $V_{\rm sEEH}(r, q, \alpha)$. We display three scalar potentials $V_{\rm sEEH}(r, q, \alpha)$ for $q = 0.5, 2, 20$ in Fig. 7 for $l = 0$(s-mode) scalar around the $n = 0$ branch, showing small negative regions near the horizon. However, this does not imply that the $n = 0$ branch is unstable against the s-mode of perturbed scalar because the sufficient condition for tachyonic instability [28] is given by $\int_{r_+}^{\infty} dr[e^{\delta} V_{\rm sEEH}(r, q, \alpha)/N(r)] < 0$. It suggests that the $n = 0$ branch may be stable against the s-mode scalar perturbation.

We have to solve Eq.(38) with two boundary conditions to test the stability of scalarized

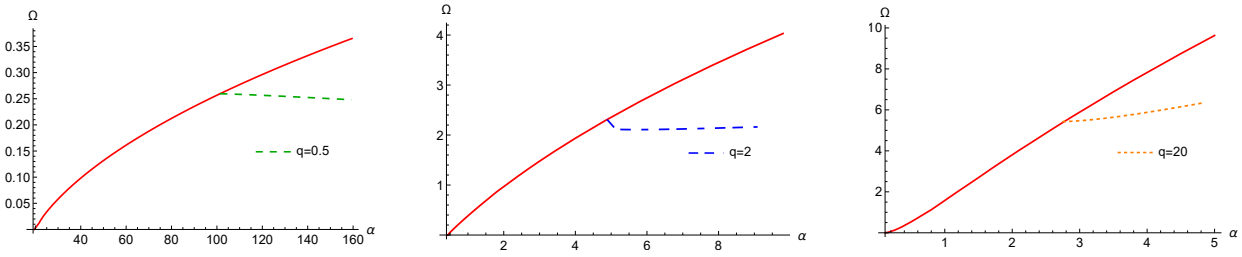

Figure 9: Positive Ω is given as a function of α for the $l = 0$ scalar mode around the $n = 1$ branch, showing instability. Here, we consider three different cases of $q = 0.5$, 2, and 20. Three dotted curves start from the $n = 1$ branch points of $\alpha_{n=1} = 101.40(q = 0.5)$, $4.888(q = 2)$, and $2.741(q = 20)$. Three red lines represent the unstable EEH black holes [see (Left) Fig. 4].

EEH black holes. This admits an exponentially growing mode of $e^{\Omega t}$ as an unstable mode. Actually, we confirm from Fig. 8 that the negative Ω with three different values of $q = 0.5, 2, 20$ implies stability for the $n = 0$ branch of sEEH black holes. This shows that the stability of $n = 0$ branch is independent of the magnetic charge q. Three red curves starting at $\alpha = \alpha_{\rm th} = 19.51(q = 0.5),\ 0.437(2),\ 0.1169(20)$ denote the positive Ω, indicating the unstable EEH black holes for $\alpha > \alpha_{\rm th} = 19.51(q = 0.5),\ 0.437(2),\ 0.1169(20)$ as was shown in (Left) Fig. 4.

In addition, we find from Fig. 9 that the $n = 1$ branch with $q = 0.5, 2, 20$ is unstable against radial perturbations.

6 Discussions

In this work, we have explored the spontaneous scalarization of the EEH black hole in the EEHS theory with a scalar coupling function $f(\phi) = e^{-\alpha\phi^2}$ to Maxwell term $\mathcal{F}$. In this case, there is no restiction on magentic charge q for the choice of the action parameter $\mu = 0.3$. This means that the overcharge $q > 1$ for spontaneous scalarization in the EMS theory [15] disappeared and no-scalar-haired inner horizon theorem [9] can be avoided automatically. The computational process is as follows: detecting the tachyonic instability of EEH black holes $\rightarrow$ predicting scalarized EEH black holes (bifurcation points) $\rightarrow$ obtaining the $n = 0, 1$ branches of sEEH black holes $\rightarrow$ performing the (in)stability analysis of these branches.

We first point out that the EEH black hole is unstable for $\alpha > \alpha_{\rm th}(q)$ (see Fig. 3), while it remains stable for $\alpha < \alpha_{\rm th}(q)$. The parameter $\alpha_{\rm th}(q) = \alpha_{n=0}(q)$ represents the instability threshold of the EEH black hole and marks the boundary between EEH black holes and the $n = 0$ branch of sEEH black holes. Accordingly, the $n = 0$ branch exists for any $\alpha \geq \alpha_{\rm th}(q)$. We further found that the bifurcation point $\alpha_{n=0}(q)$ grows as q decreases, implying that tachyonic instability is harder to be triggered for smaller magnetic charges. Since all sEEH black hole solutions emerge from spontaneous scalarization, we expect to obtain infinitely many branches ($n = 0, 1, 2, \cdots$). However, previous works [16, 17] indicate that all existed branches with $n \neq 0$ are unstable under radial perturbations.

Imporatntly, we have shown that when $q = 0.5, 2, 20$, the $n = 0$ branch of sEEH is stable against radial perturbations (see Fig. 8). This may be an issue worth further consideration in future work. Since the $n = 0$ branch of sEEH is stable for $q = 0.5, 2, 20$, and its observational implications may therefore arise [31]. On the other hand, it is worth noting that a negative potential-induced scalarization of EEH black hole has led to a single branch of unstable scalarized EEH black holes [19].

Finally, we found from Fig. 9 that the $n = 1$ branch with $q = 0.5, 2, 20$ is unstable against radial perturbations. Hence, we may deduce that all existed branches with $n \neq 0$ are unstable under radial perturbations.

Acknowledgments

Y.S.M. was supported by the National Research Foundation of Korea (NRF) grant funded by the Korea government(MSIT) (RS-2022-NR069013). D.C.Z was supported by the National Natural Science Foundation of China (NNSFC) (Grant No.12365009).

References

[1] R. Ruffini and J. A. Wheeler, Phys. Today **24**, no. 1, 30 (1971). doi:10.1063/1.3022513

[2] C. A. R. Herdeiro and E. Radu, Int. J. Mod. Phys. D **24**, no. 09, 1542014 (2015) doi:10.1142/S0218271815420146 [arXiv:1504.08209 [gr-qc]].

[3] N. M. Bocharova, K. A. Bronnikov and V. N. Melnikov, Vestn. Mosk. Univ. Ser. III Fiz. Astron. , no. 6, 706 (1970).

[4] J. D. Bekenstein, Annals Phys. **82**, 535 (1974). doi:10.1016/0003-4916(74)90124-9

[5] G. W. Gibbons and K. i. Maeda, Nucl. Phys. B **298**, 741 (1988). doi:10.1016/0550-3213(88)90006-5

[6] D. Garfinkle, G. T. Horowitz and A. Strominger, Phys. Rev. D **43**, 3140 (1991) Erratum: [Phys. Rev. D **45**, 3888 (1992)]. doi:10.1103/PhysRevD.43.3140, 10.1103/PhysRevD.45.3888

[7] G. W. Gibbons, Nucl. Phys. B **207**, 337 (1982). doi:10.1016/0550-3213(82)90170-5

[8] C. N. Pope, D. O. Rohrer and B. F. Whiting, Phys. Rev. D **110** (2024) no.10, 104036 doi:10.1103/PhysRevD.110.104036 [arXiv:2405.11042 [hep-th]].

[9] R. G. Cai, L. Li and R. Q. Yang, JHEP **03** (2021), 263 doi:10.1007/JHEP03(2021)263 [arXiv:2009.05520 [gr-qc]].

[10] D. O. Devecioglu and M. I. Park, Phys. Lett. B **829** (2022), 137107 doi:10.1016/j.physletb.2022.137107 [arXiv:2101.10116 [hep-th]].

[11] O. J. C. Dias, G. T. Horowitz and J. E. Santos, JHEP **12** (2021), 179 doi:10.1007/JHEP12(2021)179 [arXiv:2110.06225 [hep-th]].

[12] D. D. Doneva and S. S. Yazadjiev, Phys. Rev. Lett. **120**, no. 13, 131103 (2018) doi:10.1103/PhysRevLett.120.131103 [arXiv:1711.01187 [gr-qc]].

[13] H. O. Silva, J. Sakstein, L. Gualtieri, T. P. Sotiriou and E. Berti, Phys. Rev. Lett. **120**, no. 13, 131104 (2018) doi:10.1103/PhysRevLett.120.131104 [arXiv:1711.02080 [gr-qc]].

[14] G. Antoniou, A. Bakopoulos and P. Kanti, Phys. Rev. Lett. **120**, no. 13, 131102 (2018) doi:10.1103/PhysRevLett.120.131102 [arXiv:1711.03390 [hep-th]].

[15] C. A. R. Herdeiro, E. Radu, N. Sanchis-Gual and J. A. Font, Phys. Rev. Lett. **121**, no. 10, 101102 (2018) doi:10.1103/PhysRevLett.121.101102 [arXiv:1806.05190 [gr-qc]].

[16] Y. S. Myung and D. C. Zou, Eur. Phys. J. C **79**, no.3, 273 (2019) doi:10.1140/epjc/s10052-019-6792-6 [arXiv:1808.02609 [gr-qc]].

[17] Y. S. Myung and D. C. Zou, Phys. Lett. B **790**, 400-407 (2019) doi:10.1016/j.physletb.2019.01.046 [arXiv:1812.03604 [gr-qc]].

[18] Y. S. Myung and D. C. Zou, Eur. Phys. J. C **79**, no.8, 641 (2019) doi:10.1140/epjc/s10052-019-7176-7 [arXiv:1904.09864 [gr-qc]].

[19] H. Guo, M. Park and Y. S. Myung, [arXiv:2508.16083 [gr-qc]].

[20] Y. S. Myung and D. C. Zou, Phys. Rev. D **103**, no.2, 024010 (2021) doi:10.1103/PhysRevD.103.024010 [arXiv:2011.09665 [gr-qc]].

[21] L. Zhang, Q. Pan, Y. S. Myung and D. C. Zou, Phys. Rev. D **110**, no.12, 124036 (2024) doi:10.1103/PhysRevD.110.124036 [arXiv:2409.11669 [gr-qc]].

[22] H. Yajima and T. Tamaki, Phys. Rev. D **63**, 064007 (2001) doi:10.1103/PhysRevD.63.064007 [arXiv:gr-qc/0005016 [gr-qc]].

[23] D. Amaro and A. Macías, Phys. Rev. D **102**, no.10, 104054 (2020) doi:10.1103/PhysRevD.102.104054

[24] N. Bretón and L. A. López, Phys. Rev. D **104**, no.2, 024064 (2021) doi:10.1103/PhysRevD.104.024064 [arXiv:2105.12283 [gr-qc]].

[25] A. Allahyari, M. Khodadi, S. Vagnozzi and D. F. Mota, JCAP **02**, 003 (2020) doi:10.1088/1475-7516/2020/02/003 [arXiv:1912.08231 [gr-qc]].

[26] Y. S. Myung, [arXiv:2503.18239 [gr-qc]].

[27] Z. Luo and J. Li, Chin. Phys. C **46**, no.8, 085107 (2022) doi:10.1088/1674-1137/ac6574

[28] G. Dotti and R. J. Gleiser, Class. Quant. Grav. **22**, L1 (2005) doi:10.1088/0264-9381/22/1/L01 [arXiv:gr-qc/0409005 [gr-qc]].

[29] S. Hod, Phys. Lett. B **798** (2019), 135025 doi:10.1016/j.physletb.2019.135025 [arXiv:2002.01948 [gr-qc]].

[30] D. C. Zou and Y. S. Myung, Phys. Rev. D **102** (2020) no.6, 064011 doi:10.1103/PhysRevD.102.064011 [arXiv:2005.06677 [gr-qc]].

[31] Z. Stuchlík and J. Schee, Eur. Phys. J. C **79**, 44 (2019).